NUCLEAR XIAP: ROLES IN CELL GROWTH, DRUG RESISTANCE AND PROGNOSIS IN BREAST CANCER

Deborah Delbue[1], **Pedro Ivo Lucena**[3], **Marcela C. Robaina**[1], **João P.B. Viola**[2], **Eric W-F. Lam**[3], **Raquel C. Maia**[1], **Gabriela Nestal de Moraes**[1]

[1]Laboratório de Hemato-Oncologia Celular e Molecular; Programa de Hemato-Oncologia Molecular; INCA. Rio de Janeiro (RJ). [2]Programa de Biologia Celular, INCA, RJ.
[3]Department of Surgery and Cancer, Hammersmith Hospital, Imperial College London, UK.

Introduction. Breast cancer is the most common malignancy within women in Brazil and worldwide. Evasion from apoptosis and uncontrolled proliferation are hallmarks of this tumor, resulting in unbalanced levels of proliferation and cell death. In this context, XIAP emerges as an inhibitor of apoptosis protein (IAP) which exerts its antiapoptotic function through the binding and inhibition of caspases, as well as ubiquitination of target proteins. XIAP is mainly found at the cytoplasm of tumor and non-tumor cells, although its expression can also be detected at the nucleus in some cells types. Previous data from our group show that XIAP may be located at the cytoplasm and nucleus in breast cancer patients' samples, but the role of XIAP in different cell compartments remains unclear. **Aim:** To evaluate the impact of XIAP subcellular localization on cell proliferation, drug resistance and prognosis in breast cancer. **Results and Methods:** Our data show that XIAP expression is detected in all cell lines investigated but it can be found abundantly at the nuclear fraction in the doxorubicin resistant cells, MCF-7 Dox^R as assessed by subcellular fractionation and Western blotting (Figure 1). Through MTT (Figure 2) and clonogenic assays (Figure 3), we observed that dox treatment reduced cell viability and colony formation capacity in all cell lines studied, but not in MCF-7 Dox^R cells. Accordingly, MCF-7 Tax^R paclitaxel-resistant cells showed XIAP nuclear expression (Figure 4), confirming a possible correlation between the presence of nuclear XIAP and resistance to drugs used in the breast cancer treatment, regardless of its mechanism of action. Also, overexpression of nuclear XIAP through the transient transfection of XIAP$^{\Delta RING}$ and XIAP$^{NLS\ C\text{-}term}$ mutants (Figure 5), resulted in increased proliferative capacity of MCF-7 cells, although it could not change the cell cycle profile, as assessed by cell counting, clonogenic, cell viability, cristal violet assays and flow cytometry (Figure 6). Consistently, induction of nuclear XIAP expression promoted resistance to dox treatment, assessed by MTT, crystal violet and clonogenic assays (Figure 7), confirming our previous findings regarding the presence of XIAP in the nucleus of chemoresistant cells. Analysis of Kaplan-Meyer curves revealed that XIAP nuclear localization conferred a poor prognosis differently from cytoplasmic XIAP, which was associated with a trend of increased survival rate in hormone receptor-negative patients (Figure 8). Accordingly, cytoplasmic XIAP expression was associated with age ⩾ 50 years and T1 tumor size, known favorable prognostic factors in breast cancer (Table 1 and 2). In multivariate analyses, we found that nuclear XIAP was an independent prognostic factor in our group of hormone receptor-negative patients (Table 3). **Conclusion:** Taken together, our data show that XIAP expression can be found at different subcellular compartments in cell lines and breast cancer patients' samples. Remarkably, nuclear XIAP was associated with cell growth and drug resistance *in vitro*, as well as poor clinical outcome in hormone receptor-negative patients, leading to a more aggressive phenotype in breast cancer (Figure 9).

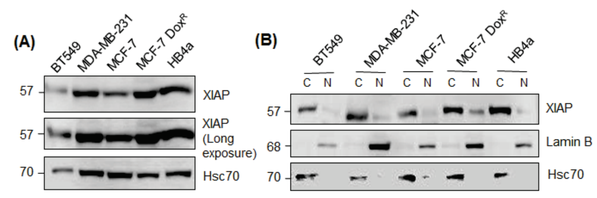

Figure 1: XIAP expression and subcellular localization in a breast-derived cell line panel . (A) The analysis of XIAP expression was performed in a panel of cell lines by Western blotting **(B)** MDA-MB-231, MCF-7, MCF-7 Dox^R, BT549 and HB4a cells were left to adhere for 24 h and then had their cytoplasmic and nuclear fractions separated by the NE-PER kit (Thermoscientific). Subsequently, XIAP expression was evaluated by Western blotting. Lamin B was used as a nuclear constitutive control, while β-tubulin as cytoplasmic constitutive control. C: cytoplasm; N: nucleus

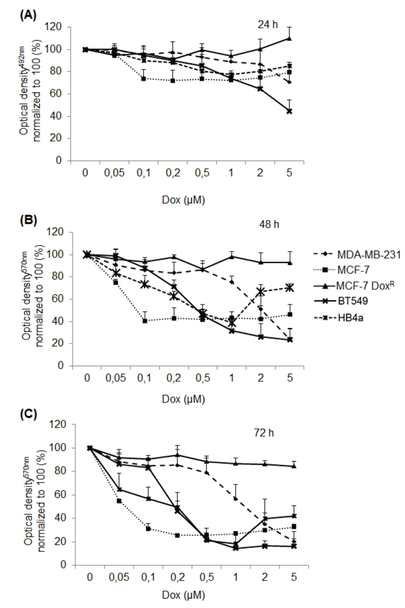

Figure 2: Cell viability profile of breast-derived cell lines following doxorubicin (dox) treatment. MDA-MB-231, MCF-7, MCF-7 Dox^R, BT549 and HB4a cells were plated in 96 well plates and left to adhere for 24 h. Subsequently, dox was added at increasing concentrations and the cells were incubated for 24 (A), 48 (B) and 72 h (C). Metabolic activity was measured by the MTT assay at 570 nm. Cell lines were compared with their control of untreated cells. The graphs correspond to the mean ± standard deviation of three independent experiments. (Student's t-test: * p <0.05; ** p <0.01; *** p <0.001; it was considered statistically significant).

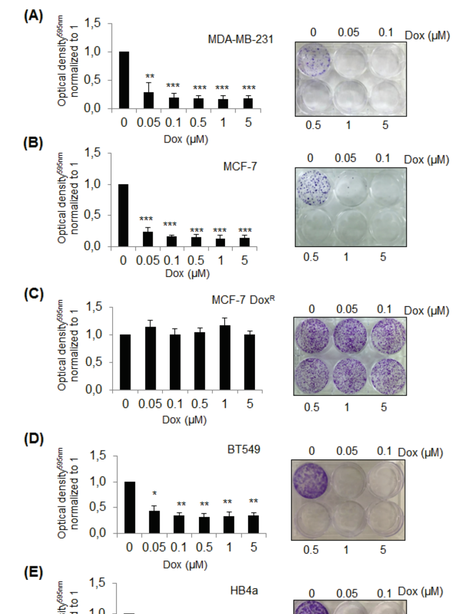

Figure 3: Changes in colony formation induced by doxorubicin (dox) in breast-derived cell lines. MDA-MB-231 **(A)**, MCF-7 **(B)**, MCF-7 Dox^R **(C)**, BT549 **(D)** and HB4a cells (E) were plated in six-well plates and left to adhere for 24 h. Subsequently, dox was added at increasing concentrations. After 48 h of drug exposure, the medium was changed and the cells were left for 14 days in the CO_2 incubator. After colony formation, cells were stained with crystal violet and has their viability measured at 595nm. The graphs correspond to the mean ± standard deviation of three independent experiments. (Student's t-test: * p <0.05; ** p <0.01; *** p <0.001; it was considered statistically significant).

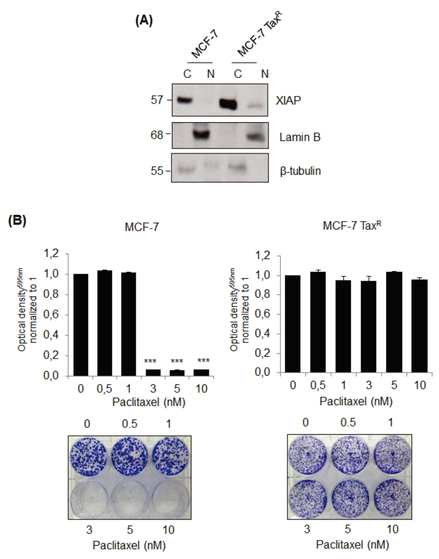

Figure 4: XIAP subcellular localization and changes in colony formation induced by paclitaxel in MCF-7 and MCF-7 Tax^R Cells were left to adhere for 24 h and then had their cytoplasmic and nuclear fractions separated by the NE-PER kit (Thermoscientific). (A) Subsequently, XIAP expression was evaluated by Western blotting. Lamin B was used as a nuclear constitutive control, while β-tubulin as cytoplasmic constitutive control. C: cytoplasm; N: nucleus. (B) Cells were plated in six-well plates and left to adhere for 24 h. Subsequently, paclitaxel was added at increasing concentrations. After 48 h of drug exposure, the medium was changed and cells were left for 14 days in the CO_2 incubator. Aftercolony formation, cells were stained with crystal violet and has their viability measured at 595nm. The graphs correspond to the mean ± standard deviation of three independent experiments. (Student's t-test: * p <0.05; ** p <0.01; *** p <0.001; it was considered statistically significant).

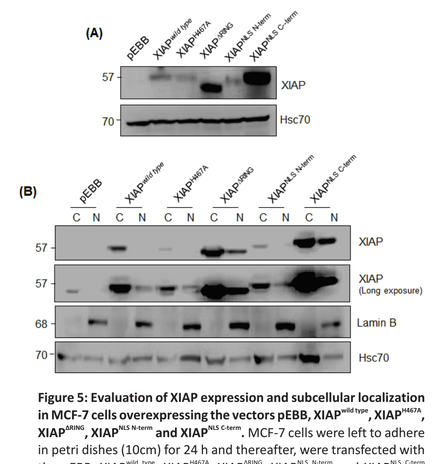

Figure 5: Evaluation of XIAP expression and subcellular localization in MCF-7 cells overexpressing the vectors pEBB, XIAP$^{wild\ type}$, XIAP^{H467A}, XIAP$^{\Delta RING}$, XIAP$^{NLS\ N\text{-}term}$ and XIAP$^{NLS\ C\text{-}term}$. MCF-7 cells were left to adhere in petri dishes (10cm) for 24 h and thereafter, were transfected with the pEBB, XIAP$^{wild\ type}$, XIAP^{H467A}, XIAP$^{\Delta RING}$, XIAP$^{NLS\ N\text{-}term}$ and XIAP$^{NLS\ C\text{-}term}$ vectors , using Lipofectamine 2000. (A) The levels of XIAP expression in XIAP-transfected cells were examined by Western blotting . (B) MCF7 cells had their cytoplasmic and nuclear fractions separated by NE-PER kit (Thermoscientific). XIAP expression was evaluated by Western blotting. Lamin B was used as a nuclear constitutive control, while β-tubulin as cytoplasmic constitutive control. C: cytoplasm; N: nucleus.

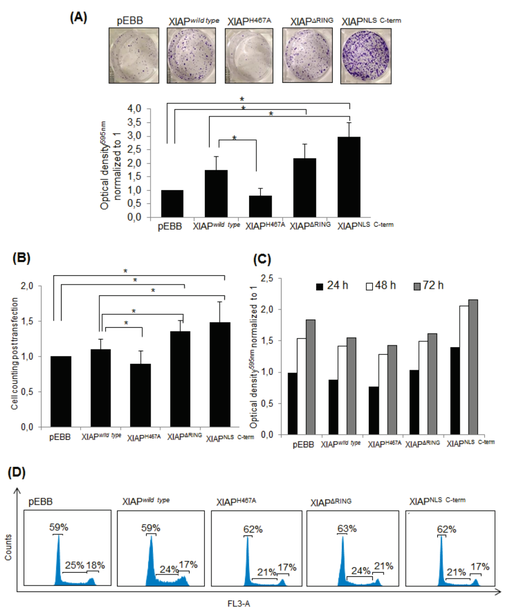

Figure 6: Effect of overexpression of XIAP and its mutants on cell growth of breast cancer cells. MCF-7 cells were left to adhere in petri dishes (10cm) or, alternatively, in 6-well plates for 24 h and thereafter, were transfected with pEBB, XIAP$^{wild\ type}$, XIAP^{H467A}, XIAP$^{\Delta RING}$ and XIAP$^{NLS\ C\text{-}term}$ vectors using Lipofectamine 2000. (A) After 24 h of transfection, MCF-7 cells were left to adhere in 6-well plates for 24 h. The cells were left for 14 days in the CO2 incubator. After colony formation, cells were stained with crystal violet and has their viability measured at 595nm. The graph corresponds to the mean and standard deviation of four independent experiments (Student t test: * p <0.05; considered statistically significant). (B) Transfected cells were counted via trypan blue exclusion 24 h post transfection. The total number of cells transfected with the empty vector (pEBB) each experiment was normalized to the value of 1. The graph corresponds to means and standard deviation of five independent experiments (Student's t test: * p <0.05; considered statistically significant). (C) Cells were transfected and left to adhere in 96-well plate. Cells were fixed and stained with crystal violet 0, 24, 48 and 72 h after adhesion and has their viability measured at 595nm. (D) The cell cycle profile of XIAP-overexpressing cells was evaluated by flow cytometry. Representative figure from two independent experiment.

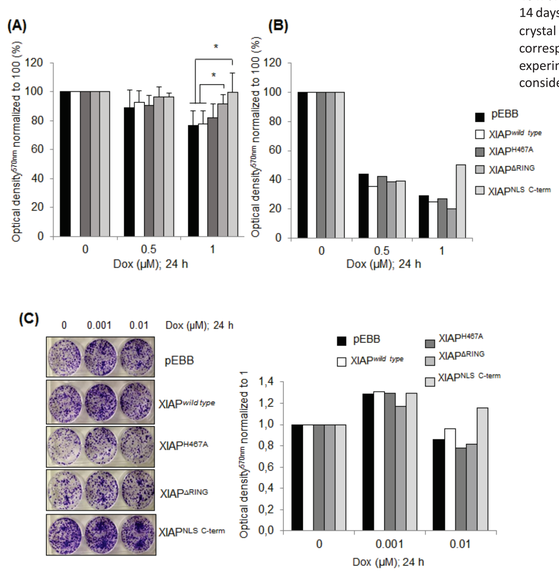

Figure 7: Effect of overexpression of XIAP and its mutants on doxorubicin (dox) resistance in breast cancer cells. MCF-7 cells were left to adhere in petri dishes (10cm) or, alternatively, in 6-well plates for 24 h and thereafter, were transfected with the vectors pEBB, XIAP$^{wild\ type}$, XIAP^{H467A}, XIAP$^{\Delta RING}$ and XIAP$^{NLS\ C\text{-}term}$, using Lipofectamine 2000. (A) After 24 h of transfection, MCF-7 cells were left to adhere in 96-well plates for 24 h. Subsequently, dox was added at 0,5 e 1 μM concentrations and the cells were incubated for 24 and 72 h for MTT and crystal violet assays. Cell viability was measured at 570nm and 595nm, respectively. For each dox concentration, the cell lines transfected with the different XIAP-encoding plasmids were compared to the XIAP wild-type transfected cells and to the empty vector pEBB. Graph A corresponds to means and standard deviation of three independent experiments (Student t test: * p <0.05, considered statistically significant). (B) Cells were transfected and left to adhere in 96-well plate. After 24, 48 and 72 h of drug exposure, they were fixed and stained with crystal violet and has their viability measured at 595nm (n=1). (C) After 24 h of transfection, MCF-7 cells were left to adhere in 6-well plates for 24 h. The cells were treat with dox for 24 h and left for 14 days in the CO_2 incubator. After colony formation, cells were stained with crystal violet and has their viability measured at 595nm (n=1).

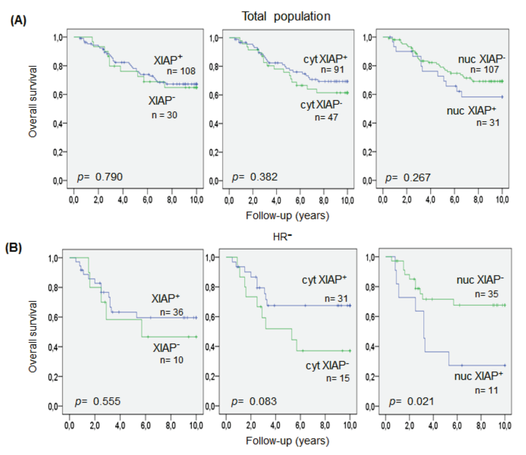

Figure 8: Overall survival of patients with infiltrating ductal breast carcinoma grouped according to total, cytoplasmic or nuclear expression of XIAP. The impact of XIAP expression and subcellular localization was analyzed in the total population (A) and in hormone receptor-negative (B) and positive (C) subgroups. The Kaplan-Meier curves, were compared by the log-rank test, where the value of p <0.05 was considered statistically significant. HR: Hormone Receptors; Cyt: cytoplasmic; Nuc: Nuclear.

Figure 9: Association between the nuclear localization of XIAP and its oncogenic role in breast cancer. XIAP expression can be found in different subcellular compartments in breast cancer cell lines and patient samples. XIAP expression in the nucleus is associated with a drug resistance phenotype and an increase in proliferative capacity in vitro. In addition, the presence of XIAP in the nucleus confers an unfavorable prognosis to patients with hormone-negative breast cancer, pointing to an oncogenic role of nuclear XIAP.

Table 3: Multivariate analysis of XIAP expression and localization in patients with infiltrating ductal breast carcinoma according to clinical-biological parameters

Total population

	Multivariate analysis		
Characteristics	***p***	**HR**	**(95% CI)**
Age at diagnosis	0.814	0.055	(0.964 - 1.048)
Tumor size	0.631	0.231	(0.583 - 1.386)
Tumor grade	0.340	0.912	(0.686 - 2.987)
Her2 expression	0.161	1.964	(0.556 - 34.298)
Hormone receptors	0.023 *	5.167	(1.140 - 5.878)
Total XIAP expression	0.756	0.097	(0.264 - 6.333)
Cytoplasmic XIAP	0.720	0.128	(0.334 - 4.894)
Nuclear XIAP	0.358	0.846	(0.175 - 1.875)

Hormone receptor-positive patients

	Multivariate analysis		
Characteristics	***p***	**HR**	**(95% CI)**
Age at diagnosis	0.569	0.569	(0.933 -1.039)
Tumor size	0.767	0.088	(0.640 - 1.389)
Tumor grade	0.498	0.459	(0.504 - 4.089)
Her2 expression	0.986	0.000	(0.000 -)
Total XIAP expression	0.406	0.691	(0.024 - 4.503)
Cytoplasmic XIAP	0.554	0.351	(0.198 - 20.574)
Nuclear XIAP	0.567	0.328	(0.231 - 14.459)

Hormone receptor-negative patients

	Multivariate analysis		
Characteristics	***p***	**HR**	**(95% CI)**
Age at diagnosis	0.409	0.682	(0.957 - 1.114)
Tumor size	0.206	1.600	(0.181 - 1.446)
Tumor grade	0.061	3.497	(0.910 - 55.629)
Her2 expression	0.560	0.340	(0.184 - 22.867)
Total XIAP expression	0.326	0.966	0.223 - 92.968)
Cytoplasmic XIAP	0.669	0.183	(0.174 - 15.216)
Nuclear XIAP	0.011 *	6.504	(0.004 - 0.483)

p< 0.05; statistically significant; HR: Hazard ratio; CI: Confidence interval

Table 1: Analysis of the association of XIAP expression and localization with clinical-biologicalparameters in hormone receptor- positive patients

	Hormone receptor-positive patients								
Characteristics	**Total XIAP**			**Cytoplasmic XIAP**			**Nuclear XIAP**		
			p			*p*			*p*
Age at diagnosis	+	-	0.021*	+	-	0.027*	+	-	0.801
≥ 50	44	6		38	12		10	40	
< 50	28	14		22	20		10	32	
Tumor size			0.940			0.343			0.351
T1	14	3		13	8		6	11	
T2	43	11		11	16		10	44	
T3	10	2		7	4		3	9	
Tumor grade			0.087			0.045*			0.548
Low (I/II)	48	10		42	16		10	48	
High (III)	16	9		12	13		6	19	
Nodal involvement			0.681			0.415			0.333
1 - 3	15	3		9	5		2	16	
4 - 9	12	1		38	2		3	10	
≥ 10	11	1		8	5		4	8	
Vascular invasion			1.000			1.000			0.152
Yes	29	8		24	13		7	30	
No	21	6		17	10		10	17	
Her2 expression			0.582			0.159			1.000
Yes	5	0		5	0		1	4	
No	67	20		55	32		19	68	

p< 0.05; statistically significant

Table 2: Analysis of the association of XIAP expression and localization with clinical-biological parameters in hormone receptor- negative patients

	Hormone receptor-negative patients								
Characteristics	**Total XIAP**			**Cytoplasmic XIAP**			**Nuclear XIAP**		
			p			*p*			*p*
Age at diagnosis	+	-	0.476	+	-	1.000	+	-	0.732
≥ 50	19	7		17	9		7	19	
< 50	17	3		14	6		4	16	
Tumor size			0.086			0.543			0.016*
T1	8	1		5	2		5	4	
T2	14	8		3	10		2	20	
T3	7	0		2	1		3	4	
Tumor grade			0.284			1.000			0.062
Low (I/II)	17	3		13	7		7	13	
High (III)	15	7		15	7		2	20	
Nodal involvement			0.725			0.218			0.786
1 – 3	5	2		7	2		2	5	
4 – 9	5	2		12	4		3	4	
≥ 10	2	2		6	2		1	3	
Vascular invasion			0.651			0.245			0.390
Yes	11	4		8	7		5	10	
No	13	2		12	3		2	13	
Her2 expression			0.284			0.243			0.658
Yes	7	1		7	1		1	7	
No	29	9		24	14		10	28	

p< 0.05; statistically significant

Financial Support: Ministério da Saúde/MS; Programa de Oncobiologia - UFRJ/Fundação do Câncer; CNPq; FAPERJ.

Projeto Gráfico: Setor de Edição e Informação Técnico-Científica / INCA